nature neuroscience

# Chronic alcohol remodels prefrontal neurons and disrupts NMDAR-mediated fear extinction encoding

Andrew Holmes[1], Paul J Fitzgerald[1], Kathryn P MacPherson[1], Lauren DeBrouse[1], Giovanni Colacicco[1], Shaun M Flynn[1,2], Sophie Masneuf[1], Kristen E Pleil[3], Chia Li[3], Catherine A Marcinkiewcz[3], Thomas L Kash[3], Ozge Gunduz-Cinar[1,2] & Marguerite Camp[1]

**Alcoholism is frequently co-morbid with post-traumatic stress disorder, but it is unclear how alcohol affects the neural circuits mediating recovery from trauma. We found that chronic intermittent ethanol (CIE) impaired fear extinction and remodeled the dendritic arbor of medial prefrontal cortical (mPFC) neurons in mice. CIE impaired extinction encoding by infralimbic mPFC neurons *in vivo* and functionally downregulated burst-mediating NMDA GluN1 receptors. These findings suggest that alcohol may increase risk for trauma-related anxiety disorders by disrupting mPFC-mediated extinction of fear.**

Alcoholism and anxiety disorders are some of the most commonly occurring neuropsychiatric disorders and often co-occur in the same individuals. Current theories emphasize the occurrence of anxiety symptoms arising as a result of a history of heavy drinking. By comparison, little attention has been paid to the effects of alcohol abuse on the subsequent risk for anxiety disorders such as post-traumatic stress disorder even though excessive drinking increases exposure to traumas such as car accidents and domestic violence[1].

Fear extinction, the learned inhibition of a trauma-related fear response, provides a valuable assay for translational studies of post-traumatic stress disorder. Studies in rodents have found evidence of impaired extinction following acute[2,3] or repeated[4,5] alcohol exposure but have been unable to clearly parse effects of alcohol on extinction from fear *per se* and have not established the mechanisms involved. In this context, fear extinction heavily recruits analogous regions of the mPFC across species[6]. In rodents, infralimbic inactivation[7], stress-induced infralimbic neuronal atrophy[8], or blockade of mPFC NMDA receptors (NMDARs)[9] and downstream signaling pathways[10] impairs fear extinction, whereas activation of the prelimbic cortex correlates with poor extinction[11,12] and prelimbic cortex inactivation reduces fear expression[7]. Although extinction deficits have not yet been reported in alcoholism, alcoholics exhibit deficits in PFC-mediated cognitive and executive functions[13] that are coupled with abnormalities in PFC volume, gray matter and activation[14]. Together, these prior observations lead to the hypothesis that chronic alcohol impairs extinction by disrupting mPFC function.

To test this idea, we subjected mice to a regimen of CIE exposure and withdrawal that was designed to mimic the repeated cycles of heavy abuse typical of alcoholism and that drive neural adaptations in circuits regulating higher order behaviors. Mice received continuous vaporized alcohol (yoked controls received vaporized air) for 16 h (to achieve 175 ± 25 mg dl$^{-1}$ in blood; **Supplementary Fig. 1**), followed by 8-h withdrawal every day for 4 consecutive days. After an 80-h withdrawal, the 4-d cycle was repeated for a total of four cycles. Mice were trained to fear an auditory conditioned stimulus repeatedly paired with foot shock 2 d after CIE to avoid nonspecific behavioral disturbances during acute withdrawal. Extinction acquisition was tested the next day (3 d post-CIE) via 50 conditioned stimulus alone presentations. To evaluate the strength of the extinction memory, we conducted a retrieval test 1 d later, followed by a context-renewal test. Conditioned stimulus–related freezing was measured as an index of fear.

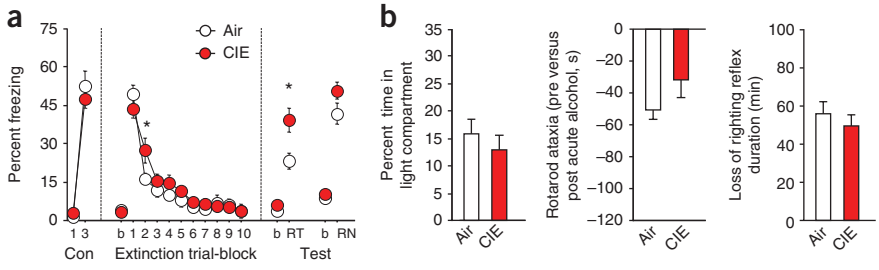


**Figure 1** CIE impairs fear extinction. (**a**) CIE transiently retarded extinction acquisition (higher fear on trial block 2) and significantly impaired extinction retrieval relative to air controls (air, $n = 10$ mice; CIE, $n = 12$ mice). b, baseline; Con, conditioning; RN, renewal; RT, retrieval. *$P < 0.05$ CIE versus air. (**b**) CIE did not affect anxiety-like behavior in the light-dark exploration test (transitions: air, 19.8 ± 10.1; CIE, 13.8 ± 2.2; $P > 0.05$) or produce tolerance to the effects of acute alcohol challenge, as measured by rotarod ataxia (pre versus post acute alcohol; **Supplementary Fig. 8**) and the loss of righting reflex (air, $n = 10$ mice; CIE, $n = 12$ mice). Data are presented as means ± s.e.m.

[1]Laboratory of Behavioral and Genomic Neuroscience, National Institute on Alcohol Abuse and Alcoholism, US National Institutes of Health, Bethesda, Maryland, USA. [2]Center for Neuroscience and Regenerative Medicine at the Uniformed Services University of the Health Sciences, Bethesda, Maryland, USA. [3]Department of Pharmacology, Bowles Center for Alcohol Studies, University of North Carolina, Chapel Hill, North Carolina, USA. Correspondence should be addressed to A.H. (andrew.holmes@nih.gov).

Received 14 June; accepted 2 August 2012; published online 2 September 2012; doi:10.1038/nn.3204

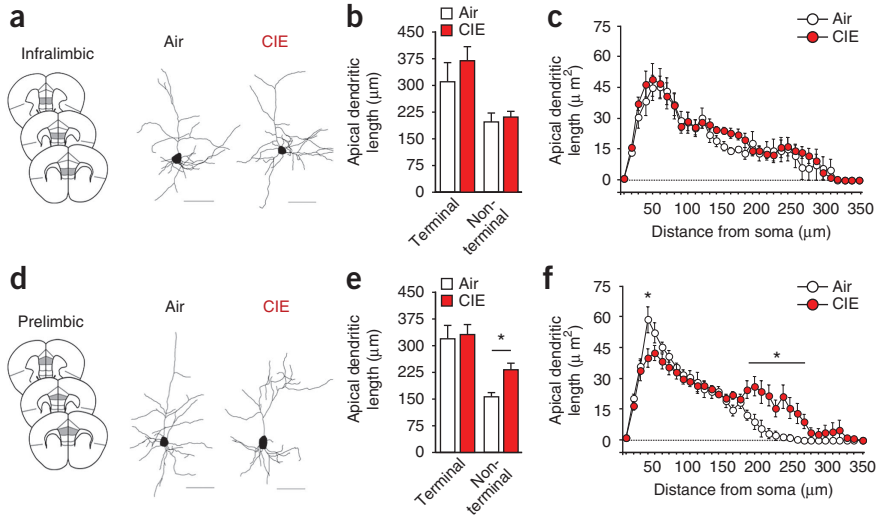


**Figure 2** CIE remodels mPFC neurons. (**a**) Coronal cartoon of infralimbic cortex. Examples of reconstructed neurons are shown. Scale bar represents 50 μm. (**b**) CIE did not alter the overall infralimbic apical length (air, $n = 7$ mice; CIE, $n = 9$ mice; $n = 6$–8 neurons per mouse for **b**,**c**). (**c**) Sholl analysis found no alcohol-induced change in infralimbic dendritic length as a function of distance from the soma. (**d**) Coronal cartoon of prelimbic cortex. Examples of reconstructed neurons. (**e**) CIE increased the overall length of prelimbic cortex apical dendrites at non-terminal branches (air, $n = 7$ mice; CIE, $n = 9$ mice; $n = 6$–8 neurons per mouse for **e**,**f**). $^*P < 0.05$ CIE versus air. (**f**) Sholl analysis revealed that prelimbic cortex apical dendritic length was shorter close to the soma and longer farther from the soma after CIE. Data are presented as means ± s.e.m. Scale bars represent 50 μm.

CIE and air groups had equivalent freezing during conditioning and the first trial block of extinction, indicating that, unlike acute alcohol[2], CIE did not disrupt fear memory formation or expression. During extinction training, both groups showed clear decreases in freezing, but CIE mice had higher freezing during the second trial block, indicating a modest retardation of extinction learning (CIE × trial-block ANOVA interaction, $F_{9,225} = 2.43$, $P < 0.01$, *post hoc* $P < 0.05$; **Fig. 1a**). Notably, however, CIE significantly impaired extinction retention, as evidenced by higher fear relative to air controls during extinction retrieval (*t* test, $t = 2.07$, degrees of freedom (df) = 25, $P < 0.05$; **Fig. 1a**). Both groups exhibited fear renewal, although this trended (*t* test, $t = 1.51$, df = 25, $P = 0.15$) higher in the CIE group. In a separate cohort of mice, CIE did not alter unconditioned anxiety-like behavior in the light-dark test (2 d post-CIE; *t* test, $t = 0.84$, df = 24, $P = 0.41$; **Fig. 1b**) and did not produce tolerance to the rotarod-ataxic (*t* test: $t = 1.40$, df = 24, $P = 0.18$) or loss of righting reflex (*t* test: $t = 0.78$, df = 24, $P = 0.44$) effects of acute alcohol challenge (3–4 d post-CIE; **Fig. 1b**). These results indicate that CIE impaired extinction, and did so in the absence of alterations in fear, anxiety or tolerance, at least on the tests employed.

Because impaired extinction is associated with altered dendritic morphology in mPFC neurons[15], we sacrificed behaviorally naive mice 3 d after CIE for visualization of infralimbic and prelimbic cortex dendritic arbors from Golgi-Cox–impregnated tissue. In infralimbic pyramidal neurons, dendritic arborization was not different between groups in the apical (ANOVA distance from soma effect, $F_{34,476} = 3009.58$, $P < 0.01$; CIE effect, $F_{1,14} = 0.38$, $P = 0.55$; **Fig. 2a–c**) or basilar (**Supplementary Fig. 2a**,**b**) tree. By contrast, prelimbic cortex neurons of CIE mice had significantly longer dendrites than did air controls in the apical (**Fig. 2d**,**e**), but not basilar (**Supplementary Fig. 2c**,**d**), tree. Furthermore, this increase was limited to non-terminal branches (*t* test, $t_{14} = 3.83$, $P < .01$) and to branches relatively distal to the soma, with a corresponding degree of dendritic retraction near the soma (ANOVA CIE × distance interaction, $F_{34,476} = 3.81$, $P < 0.01$, *post hoc* $P < 0.05$; **Fig. 2f**). Thus, CIE produced significant dendritic remodeling in mPFC neurons, which was characterized by prelimbic cortex hypertrophy. Underscoring the specificity of remodeling, we observed normal dendritic arborization after CIE in other cortical regions (orbitofrontal cortex; **Supplementary Fig. 3**) and nodes in the extinction circuit (basolateral amygdala; **Supplementary Fig. 4**).

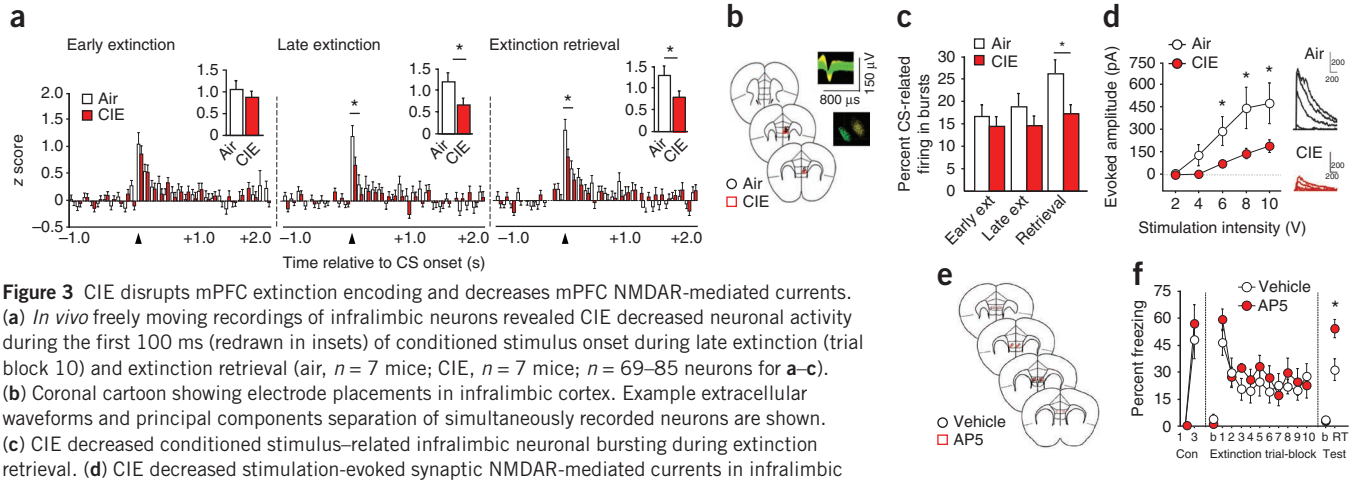


**Figure 3** CIE disrupts mPFC extinction encoding and decreases mPFC NMDAR-mediated currents. (**a**) *In vivo* freely moving recordings of infralimbic neurons revealed CIE decreased neuronal activity during the first 100 ms (redrawn in insets) of conditioned stimulus onset during late extinction (trial block 10) and extinction retrieval (air, $n = 7$ mice; CIE, $n = 7$ mice; $n = 69$–85 neurons for **a**–**c**). (**b**) Coronal cartoon showing electrode placements in infralimbic cortex. Example extracellular waveforms and principal components separation of simultaneously recorded neurons are shown. (**c**) CIE decreased conditioned stimulus–related infralimbic neuronal bursting during extinction retrieval. (**d**) CIE decreased stimulation-evoked synaptic NMDAR-mediated currents in infralimbic neurons, with example traces (air, $n = 7$; CIE, $n = 8$). (**e**) Coronal cartoon showing cannula placements in infralimbic cortex. (**f**) NMDAR antagonist AP5 infused into infralimbic cortex immediately after extinction training impaired extinction retrieval in alcohol-naive mice (air, $n = 8$; CIE, $n = 7$). Data are presented as means ± s.e.m. $^*P < 0.05$.

Dendritic dysmorphology represents a structural correlate of the CIE-induced extinction deficit but does not reveal changes in mPFC neuronal function. To more directly examine function, we performed *in vivo* neuronal recordings from multichannel electrode arrays (**Fig. 3a–c**). In rat mPFC, an extinction-encoding neuronal signal is characterized by a rapid and transient increase in firing[16]. Replicating this pattern in mice, we observed a 100-ms increase in conditioned stimulus–related firing during early extinction in infralimbic (ANOVA time effect, $F_{29,4466} = 7.81$, $P < 0.01$; **Fig. 3a**, see **Fig. 3b** for a coronal cartoon showing electrode placements) and prelimbic cortex (ANOVA time effect, $F_{29,7192} = 13.47$, $P < 0.01$; **Supplementary Fig. 5a**; see **Supplementary Fig. 5b** for a coronal cartoon showing electrode placements). This was equivalent between the air and CIE groups. Conditioned stimulus–related firing was also evident during late extinction and, more strongly still, extinction retrieval, but was significantly attenuated after CIE during both late extinction (ANOVA: infralimbic cortex, CIE × time interaction, $F_{29,4408} = 1.42$, $P = 0.066$; prelimbic cortex, CIE × time interaction, $F_{29,7192} = 1.89$, $P < 0.01$; *post hoc* $P < 0.05$) and retrieval (ANOVA: infralimbic cortex, CIE × time interaction, $F_{29,4118} = 1.61$, $P < 0.05$; prelimbic cortex, CIE × time interaction, $F_{29,6177} = 2.61$, $P < 0.01$; *post hoc* $P < 0.05$; **Fig. 3a** and **Supplementary Fig. 5a**). These data indicate that blunting of extinction-related neuronal encoding occurred in mPFC neurons.

CIE mice also showed significantly less conditioned stimulus–related burst activity during extinction retrieval. Notably, this was specific to the infralimbic cortex (*t* test, $t_{143} = 2.65$, $P < 0.01$; **Fig. 3c**), with no loss of bursting in the prelimbic cortex after CIE (**Supplementary Fig. 5c**). Although we did not see infralimbic versus prelimbic cortex differences in extinction-related neuronal firing *per se*, as has been seen in rats[7], the subregion dissociation in bursting fits well with the prior observation that low bursting in infralimbic, but not prelimbic, cortex predicts poor extinction retrieval[9].

Post-extinction training antagonism of NMDARs in infralimbic cortex impairs extinction retrieval in tandem with reduced infralimbic neuronal bursting[9], whereas chronic NMDAR blockade produces prelimbic cortex apical dendritic hypertrophy[17] similar to that produced by CIE. This suggests that CIE may cause a loss of mPFC NMDARs. Consistent with this, we found significantly reduced expression of the functionally obligatory GluN1 NMDAR subunit in mPFC tissue (infralimbic + prelimbic cortex) 3 d after CIE (air, 100 ± 8%; CIE, 61 ± 10% normalized to air; *t* test, $t_{14} = 2.96$, $P < 0.01$; **Supplementary Fig. 6**). PSD-95 and other NMDAR subunits showed normal expression, indicating no general loss of mPFC synapses (**Supplementary Fig. 6**). Furthermore, *ex vivo* slice physiology analysis revealed diminished stimulation-evoked excitatory NMDAR-mediated currents in infralimbic and prelimbic cortex neurons at the same time point post-CIE (ANOVA: infralimbic cortex, CIE × stimulation interaction, $F_{4,52} = 3.94$, $P < 0.01$, *post hoc* $P < 0.05$; prelimbic cortex, CIE × trial-block interaction, $F_{4,48} = 3.77$, $P < 0.01$; **Fig. 3d** and **Supplementary Fig. 5d**). Finally, in alcohol-naive mice, local bilateral micro-infusion of the NMDAR antagonist D(−)-2-amino-5-phosphonovaleric acid (AP5, 1 µg, 0.1 µl per side) immediately after extinction training mimicked the extinction retrieval deficit produced by CIE ($t_{13} = 2.90$, $P < 0.05$; **Fig. 3e**,**f**).

Collectively, these data propose a model in which CIE drives NMDAR downregulation in mPFC, with attendant abnormalities in dendritic morphology and neuronal encoding of extinction. A threshold of chronicity appears to be necessary to produce these effects, as subchronic CIE (two cycles) was insufficient to induce downregulation of mPFC NMDAR expression, alter infralimbic/prelimbic cortices' dendritic morphology or impair extinction (**Supplementary Fig. 7**). The finding that mPFC-mediated extinction is vulnerable to CIE implies that a chronic history of alcohol abuse may increase the risk of persistent fear after psychological trauma by degrading PFC-mediated capacity for extinction.

## METHODS

Methods and any associated references are available in the online version of the paper.

### ACKNOWLEDGMENTS

We thank Y. Shaham and C. Wellman for valuable comments, and B. Hurd, A. Plitt, D. Fisher and R. Daut for assistance with the CIE procedure. This work was supported by the US Department of Defense in the Center for Neuroscience and Regenerative Medicine (A.H., S.M.F. and O.G.-C.), US National Institutes of Health grants AA019454, AA017668 and AA020911 to T.L.K., C.L. and C.A.M., and AA021043 to K.E.P., US Department of Defense grant PT090344 (T.L.K. and K.E.P.), US National Alliance for Research on Schizophrenia and Depression (T.L.K.), Bowles Center for Alcohol Studies (T.L.K.), and the US National Institute on Alcohol Abuse and Alcoholism Intramural Research Program (A.H., P.J.F., K.P.M., L.D., S.M., G.C., O.G.-C. and M.C.).

### AUTHOR CONTRIBUTIONS

A.H., P.J.F., T.L.K. and M.C. designed the experiments. P.J.F., K.P.M., L.D., G.C., S.M.F., S.M., K.E.P., C.L., C.A.M., T.L.K., O.G.-C. and M.C. collected the data. A.H., P.J.F., K.P.M., L.D., G.C., S.M.F., S.M., K.E.P., C.L., C.A.M., T.L.K., O.G.-C. and M.C. analyzed the data. A.H. wrote the manuscript.

### COMPETING FINANCIAL INTERESTS

The authors declare no competing financial interests.

Published online at http://www.nature.com/doifinder/10.1038/nn.3204.
Reprints and permissions information is available online at http://www.nature.com/reprints/index.html.

1. WHO. *World Health Report 2006: Working Together for Health* (WHO, Geneva, 2006).
2. Lattal, K.M. *Behav. Neurosci.* **121**, 1280–1292 (2007).
3. Baum, M. *J. Comp. Physiol. Psychol.* **69**, 238–240 (1969).
4. Ripley, T.L., O'Shea, M. & Stephens, D.N. *Eur. J. Neurosci.* **18**, 441–448 (2003).
5. Bertotto, M.E., Bustos, S.G., Molina, V.A. & Martijena, I.D. *Neuroscience* **142**, 979–990 (2006).
6. Milad, M.R. *et al. Biol. Psychiatry* **66**, 1075–1082 (2009).
7. Sierra-Mercado, D., Padilla-Coreano, N. & Quirk, G.J. *Neuropsychopharmacology* **36**, 529–538 (2011).
8. Izquierdo, A., Wellman, C.L. & Holmes, A. *J. Neurosci.* **26**, 5733–5738 (2006).
9. Burgos-Robles, A., Vidal-Gonzalez, I., Santini, E. & Quirk, G.J. *Neuron* **53**, 871–880 (2007).
10. Herry, C., Trifilieff, P., Micheau, J., Luthi, A. & Mons, N. *Eur. J. Neurosci.* **24**, 261–269 (2006).
11. Burgos-Robles, A., Vidal-Gonzalez, I. & Quirk, G.J. *J. Neurosci.* **29**, 8474–8482 (2009).
12. Whittle, N., Hauschild, M., Lubec, G., Holmes, A. & Singewald, N. *J. Neurosci.* **30**, 13586–13596 (2010).
13. Goldstein, R.Z. *et al. Neuropsychologia* **42**, 1447–1458 (2004).
14. Pfefferbaum, A., Sullivan, E.V., Rosenbloom, M.J., Mathalon, D.H. & Lim, K.O. *Arch. Gen. Psychiatry* **55**, 905–912 (1998).
15. Holmes, A. & Wellman, C.L. *Neurosci. Biobehav. Rev.* **33**, 773–783 (2009).
16. Milad, M.R. & Quirk, G.J. *Nature* **420**, 70–74 (2002).
17. Martin, K.P. & Wellman, C.L. *Cereb. Cortex* **21**, 2366–2373 (2011).

## ONLINE METHODS

**Subjects.** Subjects were male C57BL/6J mice obtained at ~8 weeks of age from the Jackson Laboratory. Mice were housed two to a cage in a temperature- (72 ± 5° F) and humidity- (45 ± 15%) controlled vivarium under a 12-h light/dark cycle (lights on at 0600 h). The numbers of mice used in each experiment are given in the figure legends. All experimental procedures were approved by the National Institute on Alcohol Abuse and Alcoholism Animal Care and Use Committee and followed the US National Institutes of Health guidelines outlined in *Using Animals in Intramural Research*.

**Alcohol exposure.** Chronic alcohol exposure was achieved via a vapor inhalation procedure previously described for C57BL/6J mice[18]. Mice were placed in standard mouse cages in Plexiglas vapor chambers (60 × 36 × 60 cm, PlasLabs, up to six cages per chamber) and exposed to continuous vaporized alcohol. Alcohol was volatized by passing air through an air stone submerged in ethanol (95%) and mixed with fresh air to deliver 19–22 mg of alcohol per l of air at a rate of ~10 l $min^{-1}$. These delivery parameters were designed to produce blood alcohol levels of 175 ± 25 mg $dl^{-1}$, which was confirmed weekly via blood samples taken from dedicated 'sentinel' mice exposed to alcohol simultaneously with the test mice. To initiate intoxication and stabilize blood alcohol levels, the alcohol group received intraperitoneal injections of 1 mmol $kg^{-1}$ of the alcohol dehydrogenase inhibitor pyrazole (Sigma) combined with 1.5 g per kg of body weight of 20% alcohol (v/v), in a volume of 10 ml per kg of body weight, before placement in the chambers. Exposure lasted for 16 h each day (in at 1700 h, 2 h before start of the 12-h circadian dark phase, out at 0900 h), followed by an 8-h withdrawal. There were 4 consecutive days of intermittent exposure (Monday through Thursday) and then an 80-h withdrawal (Friday through Monday). This complete weekly cycle was repeated four times. Air controls received an injection of 1 mmol per kg of body weight pyrazole in saline to control for this treatment, before placement in dedicated air chambers (located adjacent to the alcohol chambers), which received vaporized air at the same exchange rate as the alcohol chambers.

**Fear conditioning and extinction.** Mice were fear conditioned and subsequently tested for fear extinction 2 d after the completion of alcohol exposure, using previously described procedures[19]. Testing was conducted at this time point post-alcohol to avoid confounding effects of acute physical withdrawal that have been shown to cause malaise and generalized suppression of behavior in mice tested for spontaneous activity at earlier time points (for example, 1 d after chronic alcohol)[20].

The effects of group (alcohol versus air) and trial or trial block on freezing during conditioning and extinction were analyzed using two-factor ANOVA, with repeated measures for trial or trial block, followed by Fisher's LSD *post hoc* tests. Unpaired Student's *t* tests were used to compare groups during the extinction retrieval and renewal tests. The threshold for statistical significance for this and all other analysis was set at $P < 0.05$. All data were analyzed using Statview (SAS Institute).

**Anxiety-like behavior.** Mice were tested for anxiety-like behavior using the light/dark exploration test 2 d after the completion of alcohol exposure, using previously described procedures[21]. Unpaired Student's *t* tests were used to compare groups.

**Tolerance to acute alcohol challenge.** The development of tolerance to the intoxicating effects of alcohol was assessed using two assays, ataxia and loss of righting reflex, which recruit overlapping, but dissociable, mechanisms[22]. The day after testing for anxiety-like behavior as above, mice were tested for 2.0 g per kg of body weight alcohol-induced ataxia using the accelerating rotarod as previously described[23]. Unpaired Student's *t* tests were used to compare groups. Mice were tested 1 d later for 3.5 g per kg of body weight alcohol-induced loss of righting reflex duration, as previously described[24]. Unpaired Student's *t* tests were used to compare groups.

**Neuronal dendritic morphology.** We overdosed behaviorally naive mice with xylazine/ketamine 3 d after the completion of alcohol exposure and then transcardially perfused them with 0.9% saline (w/v) to obtain brains for analysis of the dendritic morphology of pyramidal neurons in prelimbic and infralimbic cortex. Dendritic morphology was determined using Glaser and Van der Loos' modified Golgi stain, essentially as described previously[25]. The effects of group (alcohol or air) and distance from the soma on dendritic length were analyzed using two-factor ANOVA, with repeated measures for distance from the soma, followed by Fisher's LSD *post hoc* tests. Unpaired Student's *t* tests were used to compare overall apical length between groups.

***In vivo* neuronal recordings.** Mice were anesthetized with isoflurane and placed in a stereotaxic alignment system (Kopf Instruments) for implantation of a microelectrode array. The array (fabricated by Innovative Neurophysiology) comprised 16 tungsten microelectrodes (35 µm in diameter) arranged into two rows of eight microelectrodes (150-µm spacing between microelectrodes in a row, 200-µm spacing between rows). Arrays were targeted to infralimbic or prelimbic cortex, with rows running lengthwise anterior to posterior (infralimbic cortex targeting coordinates for center of array: anteroposterior (AP) +1.75–1.80, mediolateral (ML) +0.35–0.50, dorsoventral (DV) −2.90; prelimbic cortex targeting coordinates for center of array: AP +1.90, ML +0.35–0.50, DV −2.30). After 7–10 d of recovery, alcohol exposure commenced as described above.

Fear conditioning and extinction were conducted 2 d after the completion of alcohol exposure as described above, with the exception of the omission of the extinction renewal test and the addition of a pre-conditioning session (procedure as for the retrieval test, but no unconditioned stimulus (US) and in a context different from either context A or B) to measure neural responses to the conditioned stimulus. Neuronal activity was recorded during the pre-conditioning, extinction training and retrieval sessions using the Plexon Multichannel Acquisition Processor. Extracellular waveforms exceeding a set voltage threshold were digitized at 40 kHz and stored in a PC. Waveforms were manually sorted using principal component analysis of spike clusters and visual inspection of waveforms and interspike intervals. Neuronal activity was time stamped to conditioned stimulus onset, and spike and time stamp information were integrated and analyzed using NeuroExplorer (NEX Technologies).

Average neuronal activity was organized into 100-ms bins and time stamped around a 2-s epoch after conditioned stimulus onset that was compared to a 1-s pre–conditioned stimulus baseline. These data were *z* score transformed to the pre–conditioned stimulus baseline average ([conditioned stimulus activity – pre–conditioned stimulus activity]/s.d. of pre–conditioned stimulus activity) and presented in peri-event histograms. Conditioned stimulus–related neuronal bursting was calculated as previously described[9]. A burst was defined as three or more consecutive spikes with an interspike interval of <25 ms between the first two spikes and <50 ms between subsequent spikes. Bursting was expressed as the percentage of all conditioned stimulus–related spikes participating in bursts. The effects of group (alcohol versus air) and time on *z* scores during early extinction training (first block of five trials), late extinction training (last block of five trials) and extinction retrieval were analyzed using two-factor ANOVA, with repeated measures for time, followed by Fisher's LSD *post hoc* tests. Unpaired Student's *t* tests were used to compare groups for bursting.

At the completion of testing, array placement was verified by electrolytic lesions made by passing 100 µA through the electrodes for 20 s using a current stimulator (S48 Square Pulse Stimulator, Grass Technologies). Brains were removed, and 50-µm coronal sections were cut with a vibratome (Classic 1000 model, Vibratome) and stained with cresyl violet. Placement was estimated with reference to a mouse brain atlas[26] and the aid of an Olympus BX41 microscope.

**Western blotting.** Behaviorally naive mice were sacrificed via cervical dislocation and rapid decapitation 3 d after the completion of CIE. Brains were quickly removed and flash-frozen. Tissue punches from PFC were homogenized on ice by sonication in buffer (0.1% SDS (wt/vol), 1% sodium deoxycholate (wt/vol), 1% NP-40 (vol/vol), 150 mM NaCl, 25 mM Tris, pH 7.6) containing a protease inhibitor cocktail (Roche). The homogenate was centrifuged at 20,500 *g* for 10 min at 4 °C and the supernatant protein concentration was determined by Bradford Method using bovine serum albumin as a standard. Samples were mixed (1:1) with a Laemmli sample buffer and β-mercaptoethanol, and denatured by boiling for 10 min at 80 °C. Each sample containing protein from one mouse was run (10–30 µg per lane) on a 7.5% SDS-PAGE gel (Bio-Rad) and transferred to Polyvinylidene fluoride membranes (PVDF pore size 0.2 µm) with Trans-Blot SD, a semi-dry electrophoretic Transfer Cell (Bio-Rad). Blots were blocked with 5% milk (w/v) in TBST (25 mM Tris-HCl (pH 7.4), 150 mM NaCl and 0.1% Tween 20 (v/v)) for 1 h at room temperature (24 °C). Blots were washed three times




doi:10.1038/nn.3204

for 10 min with TBST and incubated overnight at 4 °C with primary antibody: antibody to GluN1 (1:150, Abcam, cat. no. AB17345, predicted molecular weight 105 kDa, observed band ~100 kDa), antibody to GluN2B (1:300, Millipore, cat. no. AB1557P, predicted molecular weight 180 kDa, observed band ~180 kDa), antibody to GluN2A (1:500, Millipore cat. no. AB1555P, predicted molecular weight 180 kDa, observed band ~180 kDa), antibody to PSD-95 (1:500, NeuroMab UC Davis/NIH NeuroMab Facility, cat. no. 75-028, NeuroMab clone K28/43, predicted band size 95-110 kDa, observed band ~95 kDa). β-actin (1:5,000, Abcam cat. no. AB8226, predicted band size 42 kDa, observed band ~50 kDa) was used as a loading control. Blots were then washed three times for 10 min in TBST, and then incubated for 1 h at room temperature (24 °C), appropriately with horseradish peroxide–conjugated donkey antibody to rabbit (Santa Cruz Biotechnologies, cat. no. SC-2077, 1:5,000) and horseradish peroxide–conjugated goat antibody to mouse IgG1 (1:5,000, Santa Cruz Biotechnologies, cat. no. SC-2969) in 5% milk in TBST. After another three washes for 10 min with TBST, immunoreactivity was detected using SuperSignal West Dura chemiluminescence detection reagent (Thermo Scientific) and collected using a Kodak Image Station 4000R. Net intensity values were determined using the Kodak MI software and were normalized to total beta actin. Unpaired Student's *t* tests were used to compare values between groups.

***Ex vivo* slice electrophysiology.** Behaviorally naive mice were overdosed with isoflurane and sacrificed via decapitation 3 d after the completion of CIE. We cut 300-μm-thick brain slices containing the mPFC using a Leica VT1200 vibratome (Leica Biosystems) and stored them in a heated, oxygenated holding chamber containing artificial cerebrospinal fluid (124 mM sodium chloride, 4.4 mM potassium chloride, 2 mM calcium chloride, 1.2 mM magnesium sulfate, 1 mM sodium phosphate, 10 mM glucose and 26 mM sodium bicarbonate) before being transferred to a submerged recording chamber maintained at approximately 30 °C (Warner Instruments). Slices were placed in a submerged chamber (Warner Instruments) and mPFC pyramidal neurons located in layers II/III and V of the infralimbic and prelimbic cortex were directly visualized with Olympus infrared video microscopy. Recording electrodes (3–6 MΩ) were pulled on a Flaming-Brown Micropipette Puller (Sutter Instruments) using thin-walled borosilicate glass capillaries.

NMDAR excitatory postsynaptic currents (EPSCs) were evoked by local fiber stimulation with bipolar nichrome electrodes. Stimulating electrodes were placed locally and electrical stimuli (2–10 V in 2-V increments, with a 100–150-μs duration) were applied at 0.2 Hz. NMDAR EPSCs were pharmacologically isolated by adding 25 μM picrotoxin and 10 μM 6-nitro-2,3-dioxo-1,4-dihydrobenzo[f]quinoxaline-7-sulfonamide (NBQX) and recorded at a holding potential of +40 mV. Recording electrodes were filled with a solution containing 135 mM cesium gluconate, 5 mM NaCl, 10 mM HEPES, 0.6 mM EGTA, 4 mM ATP, 0.4 mM GTP and 2 mM QX-314 (pH 7.2, 290–295 mOsmol). Signals were acquired via a Multiclamp 700B amplifier (Molecular Devices), digitized and analyzed via pClamp 10.2 software (Molecular Devices). NMDAR input-output curves were constructed by taking the average peak amplitude of the NMDAR EPSC at each stimulation voltage.

**Infralimbic NMDAR antagonism in alcohol-naive mice.** Via stereotaxic surgery, as above, alcohol-naive mice were implanted with a 26-gauge indwelling cannula (Plastics One) bilaterally targeting the infralimbic cortex (AP: +1.65, ML: ±0.4, DV: −2.0). Cannula tips were placed 1.0 mm above infralimbic cortex to accommodate the extension of the injector into this brain region. After 5–7 d of recovery, mice were tested for fear conditioning, extinction training and retrieval, as above, with the exception that saline vehicle or 1 μg AP5 (Tocris) was infused into infralimbic cortex within 5 min of the completion of extinction training. The post-training procedure and drug concentration followed previous studies in rats[9,27], with the injection volume (0.1 μl per side) and injection rate (0.25 μl $min^{-1}$) adapted for the smaller brain of the mouse. To ensure diffusion and reduce reflux, custom modified injector needles (1.1-mm projection beyond the cannula tip) were inserted before infusion to produce a small reservoir for the infused drug, and injectors remained in place for 5 min post-injection.

At the completion of testing, cannula placement was verified with the aid of methylene blue dye infused into infralimbic cortex. Mice were overdosed with xylazine/ketamine and transcardially perfused with 4% paraformaldehyde (w/v). Brain sections were then cut and inspected as above.


18. Becker, H.C. & Lopez, M.F. *Alcohol. Clin. Exp. Res.* **28**, 1829–1838 (2004).
19. Wellman, C.L. *et al. J. Neurosci.* **27**, 684–691 (2007).
20. Kliethermes, C.L., Cronise, K. & Crabbe, J.C. *Physiol. Behav.* **85**, 479–488 (2005).
21. Mozhui, K. *et al. J. Neurosci.* **30**, 5357–5367 (2010).
22. Crabbe, J.C., Cameron, A.J., Munn, E., Bunning, M. & Wahlsten, D. *Curr. Protoc. Neurosci.* **9**, 9.26 (2008).
23. Palachick, B. *et al. Alcohol. Clin. Exp. Res.* **32**, 1479–1492 (2008).
24. Daws, L.C. *et al. J. Neurosci.* **26**, 6431–6438 (2006).
25. Izquierdo, A., Wellman, C.L. & Holmes, A. *J. Neurosci.* **26**, 5733–5738 (2006).
26. Paxinos, K.B.J. & Franklin, G. *The Mouse Brain in Stereotaxic Coordinates* (Academic Press, London, 2001).
27. Fiorenza, N.G., Rosa, J., Izquierdo, I. & Myskiw, J.C. *Behav. Brain Res.* **232**, 210–216 (2012).